Heat Transfer Measurements and Correlations in the Transition Region for a Circular Tube with Three Different Inlet Configurations

Afshin J. Ghajar
Lap-Mou Tam
School of Mechanical and Aerospace Engineering, Oklahoma State University, Stillwater, Oklahoma

■ Local forced and mixed convective heat transfer measurements were made in a horizontal circular straight tube with reentrant, square-edged, and bell-mouth inlets under uniform wall heat flux condition. For the experiments the Reynolds number of the liquid ranged from about 280 to 49,000, the Prandtl number varied from 4 to 158, and the Grashof number ranged from about 1000 to 2.5×10^5. From the experiments the heat transfer transition Reynolds number range was determined to be about 2000–8500 for the reentrant inlet, 2400–8800 for the square-edged inlet, and 3800–10,500 for the bell-mouth inlet. A correlation for prediction of the developing and fully developed forced and mixed convection heat transfer coefficients in the transition region for each inlet is recommended. Heat transfer correlations for the laminar and turbulent regions for the three inlets are also proposed. Some of the available heat transfer correlations are compared with our experimental data for different inlets.

Keywords: *heat transfer coefficient, mixed convection, transition region, circular tube, heat exchangers*

INTRODUCTION

An important design problem in industrial heat exchangers arises when flow inside the tubes falls into the transition region. In practical engineering design, the usual recommendation is to avoid design and operation in this regime; however, this is not always feasible under design constraints. The usually cited transition Reynolds number of about 2100 applies, strictly speaking, to a very steady and uniform entry flow with a rounded entrance. If the flow has a disturbed entrance typical of heat exchangers, in which there is a sudden contraction and possibly even a reentrant entrance, the transition Reynolds number will be less.

Experimental, numerical, and analytical studies are available for forced and mixed convection heat transfer in horizontal tubes with a rounded entrance in the laminar, transitional, and turbulent flow regimes. These works have been reviewed by Shah and London [1], Shah and Johnson [2], and Kakac and coworkers [3, 4]. However, very little information that is of immediate use to a design engineer (ie, correlation) is available to predict the developing and fully developed transitional forced and mixed convection heat transfer coefficients in a tube with a disturbed entrance.

The results of the experimental forced and mixed convection heat transfer studies in the entrance and fully developed regions of a circular horizontal pipe with a rounded entrance for all three flow regimes are usually presented in the form of empirical or numerical heat transfer correlations [4]. The type of inlet configuration influences the development of the heat transfer coefficient along the pipe and the beginning and end of the transition region. Therefore, the application of these correlations to tubes with disturbed entrances should be investigated. In addition, most of the data used for the empirical correlations were obtained with fewer than four thermocouples around the periphery of the tube at each axial location along the tube. This results in neglecting the peripheral heat transfer and the inability to properly detect the occurrence of mixed convection, especially for laminar and transitional flows. Finally, some of the experiments were performed in short test sections where transitional flow was likely to have existed for at least some of the tube length.

The purpose of this study was to create an accurate and broad forced and mixed convection heat transfer database across all flow regimes for a wide range of Reynolds, Prandtl, and Grashof numbers in the entrance and fully developed regions of a circular horizontal electrically heated straight tube fitted with three different inlet configurations (reentrant, square-edged, and bell-mouth). The database was used to investigate the influence of inlet configuration on the transition region and the development of empirical heat transfer correlations for all flow regimes and inlet configurations. In addition, the database

Address correspondence to Professor A. J. Ghajar, School of Mechanical and Aerospace Engineering, Oklahoma State University, Stillwater, OK 74078.

Experimental Thermal and Fluid Science 1994; 8:79–90
© 1994 by Elsevier Science Inc., 655 Avenue of the Americas, New York, NY 10010
0894-1777/94/$7.00

was used to establish the validity of some of the available heat transfer correlations for various inlet configurations.

EXPERIMENTS

A schematic diagram of the overall experimental setup used for heat transfer experiments is shown as Fig. 1. The experimental setup shown was also used for pressure drop measurements [5]. The heat transfer test section was a horizontal seamless 316 stainless steel circular tube with an inside diameter of 1.58 cm and an outside diameter of 1.90 cm. The total length of the test section was 6.10 m, providing a maximum length-to-diameter ratio (L/D) of 385. The end connections of the test section consisted of copper plates that were arc soldered with silver to the ends of the test section to secure a well-defined electric circuit through the end plates. The test section was insulated from the environment by using fiberglass pipe insulation and vaporproof pipe tape. The total thickness of the insulation materials was about 3.18 cm. To ensure a uniform fluid bulk temperature at the exit of the test section, a mixing well that consisted of several baffles was used. A one-shell, two tube pass heat exchanger was used to cool the fluid from the test section to a desirable inlet bulk temperature.

To ensure a uniform velocity distribution in the test fluid before it entered the test section, the flow passed through a calming and inlet section (see Fig. 2). The calming section consisted of a 17.8 cm diameter acrylic plastic cylinder with three perforated acrylic plastic plates with an open area ratio of 0.312 (73 holes per plate, hole diameter 1.1 cm) followed by tightly packed soda straws (inside diameter 0.57 cm, length 10.2 cm, open area ratio 0.915) sandwiched between galvanized steel mesh screens (wire diameter 0.07 cm, mesh width 0.28 cm, open area ratio 0.597). Before leaving the calming section, test fluid passed through a fine mesh screen (wire diameter 0.03 cm, mesh width 0.14 cm, open area ratio 0.692). The total length of the calming section was 61.6 cm. Test fluid leaving the calming section entered the inlet section and flowed undisturbed through 23.5 cm of a 16.5 cm diameter acrylic plastic tube before it entered the test section. This

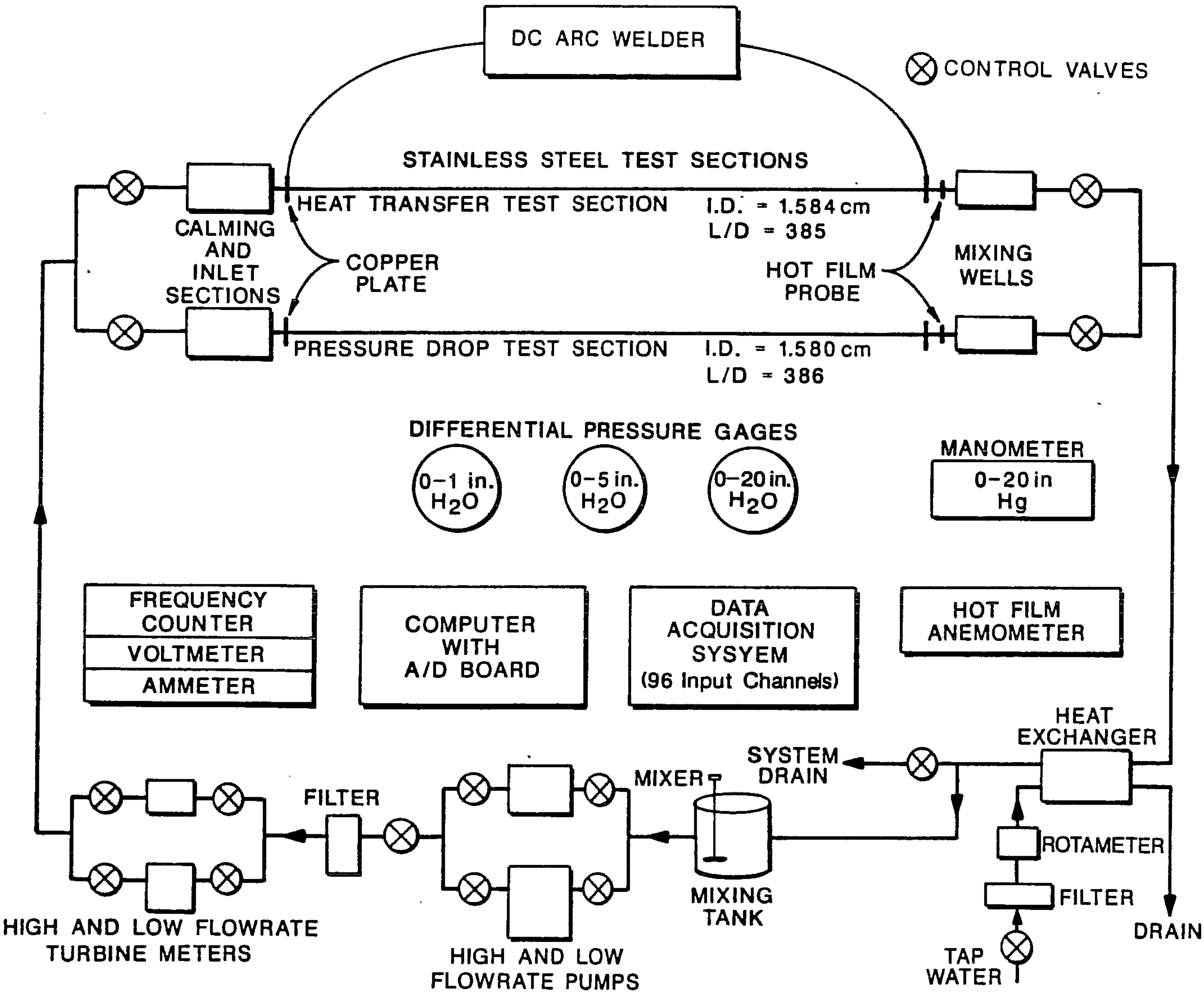

Figure 1. Schematic diagram of the experimental setup.

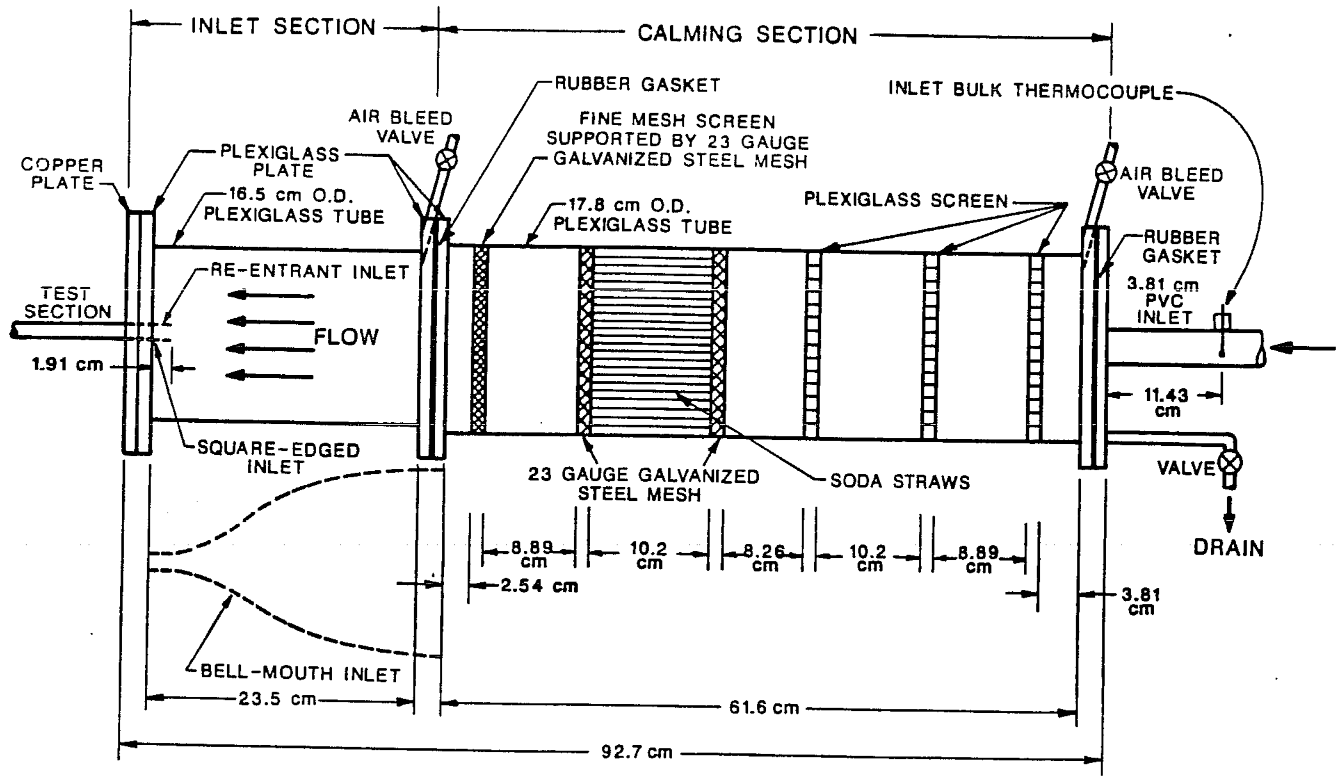

Figure 2. Schematic diagram of calming and inlet sections.

was done to ensure a uniform velocity distribution upon entering the test section. The calming and inlet sections were also equipped with air bleed valves that were used to evacuate air during startup.

The inlet section had the versatility of being modified to incorporate a reentrant or a bell-mouth entrance (see Fig. 2). The reentrant entrance was simulated by sliding 1.91 cm of the tube entrance length into the inlet section (Fig. 2), which was otherwise the square-edged (sudden contraction) entrance. For the bell-mouth entrance, a nozzle had to be constructed to replace the inlet section of Fig. 2. The nozzle was designed according to the method sug-

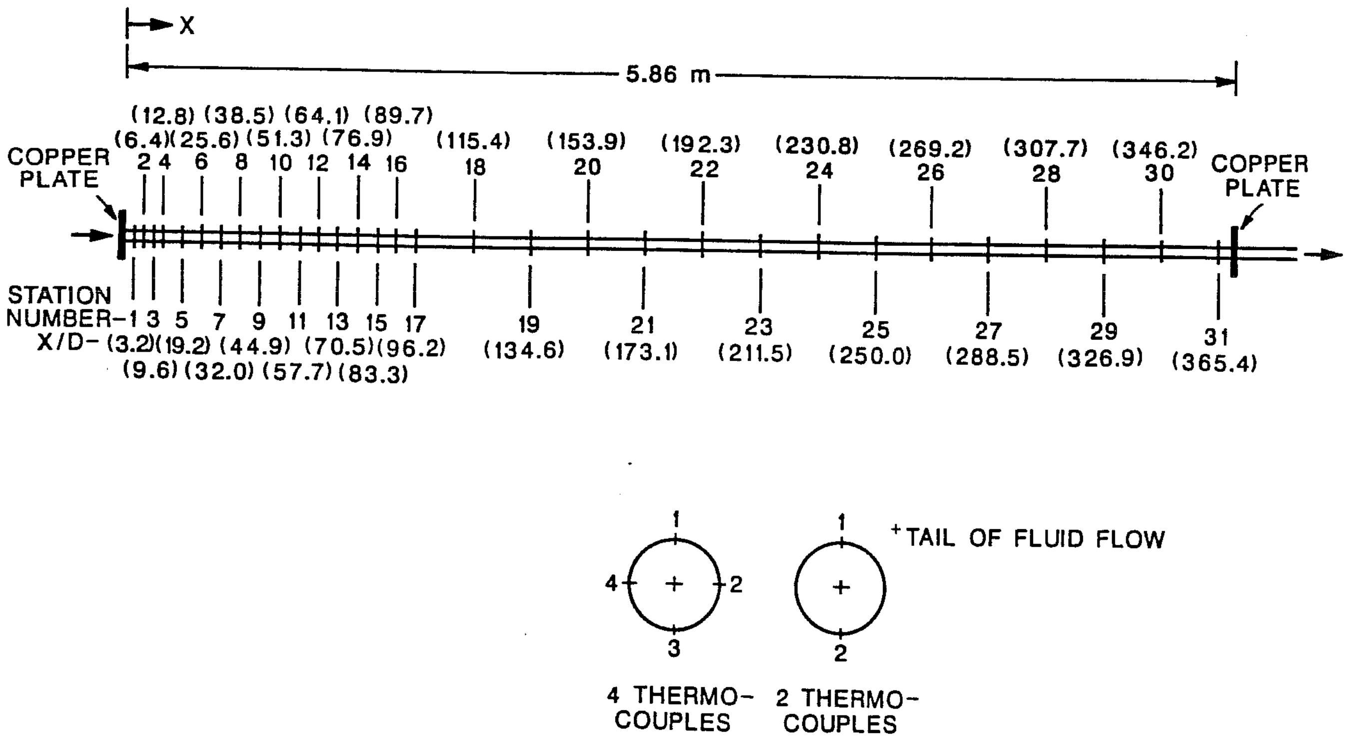

Figure 3. Heat transfer test section thermocouple distribution.

gested by Morel [6] and was constructed of fiberglass. The nozzle had a contraction ratio of 10.7 and a total length of 23.6 cm. Construction of the nozzle, a multistep process, consisted of constructing a two-dimensional contour on a numerically controlled milling machine from a computer-generated profile, using the contour and a hydraulic follower on a lathe to produce an axisymmetric male mold, and forming the fiberglass nozzle around the male mold, with aluminum flanges formed in.

A uniform wall heat flux boundary condition was maintained by a Lincoln DC-600 welder. Thermocouples were placed on the outer surface of the tube wall at close intervals near the entrance and at greater intervals further downstream (see Fig. 3 for details). Thirty-one thermocouple stations were designated with four thermocouples at each station. The thermocouples were place 90° apart around the periphery. Omega TT-T-30 copper-constantan insulated T-type thermocouples were used with Omega EXPP-T-20 extension wire for relay to the data acquisition system. The thermocouples were attached to the outside of the tube wall with Omegabond 101, an epoxy adhesive with high thermal conductivity and electrical resistivity. The inlet and exit bulk temperatures were measured by means of thermocouple probes (Omega TJ36-CPSS-14U-12) inserted in the calming section and the mixing well, respectively. Calibration of thermocouples and thermocouple probes showed that they were accurate within ± 0.4°C. The data acquisition system used for the temperature measurements consisted of a Cole-Parmer MAC-14 datalogger with 96 input channels interfaced with a personal computer. Due to the limitations of the data acquisition system, only 96 of the 124 thermocouples were used, requiring some stations and peripheral locations to be ignored during data collection. The extra unused thermocouples provide additional flexibility should insight at their location be desired. These excluded stations were number 2 and even-numbered stations 24–30 (see Fig. 3). For 21 of the 26 stations used for temperature measurements, all four thermocouples around the periphery were used; for five stations (23, 25, 27, 29, and 31), only the top and bottom thermocouples were employed. The flow rate was measured by a turbine meter located upstream from the test section. The turbine meter had a linearity of $\pm 0.5\%$ of reading and a repeatability of less than $\pm 0.10\%$ of reading. The voltage drop across the test section and the current carried by the test section were measured by a voltmeter and an ammeter, respectively.

To prevent them from transmitting noise and vibration through the experimental setup, the welder and the pumps were mounted inside a plywood box lined with insulation. For the welder, cooling air was brought in from outside the room to the welder box and exhausted outside the room through custom-made plenums. In addition, rubber hoses were connected to the pump box to present the transmission of vibration to the fluid return tubing. All equipment was placed on damping pads to prevent vibration from being transmitted through the floor.

The heat transfer measurements at uniform wall heat flux boundary condition were carried out by measuring the local outside wall temperatures at 26 stations along the axis of the tube and the inlet and outlet bulk temperatures in addition to other measurements such as the flow rate, room temperature, voltage drop across the test section, and current carried by the test section. The local peripheral heat transfer coefficient and Nusselt number were then calculated for each of these stations based on the knowledge of pipe inside wall temperature and inside wall heat flux obtained from a data reduction computer program developed exclusively for this type of experiment [7]. The local average peripheral values for inside wall temperature, inside wall heat flux, heat transfer coefficient, and Nusselt number were then obtained by averaging all the appropriate individual local peripheral values at each axial location. The computer program used a finite-difference formulation to determine the inside wall temperature and the inside wall heat flux from measurements of the outside wall temperature, the heat generation within the pipe wall, and the thermophysical properties of the pipe material (electrical resistivity and thermal conductivity). In these calculations, axial conduction was assumed negligible (RePr > 42,000 in all cases), but peripheral and radial conduction of heat in the tube wall were included. In addition, the bulk fluid temperature was assumed to increase linearly from the inlet to the outlet.

Two test fluids of different concentrations were used in the experiments. Full-strength concentrations of distilled water and ethylene glycol were followed by mixtures of 60–92% ethylene glycol and water (by mass fraction). Expressions for the physical properties of water, ethylene glycol, and ethylene glycol–water mixtures along with their accuracy and range of application are reported in Ref. 7. For the experiments, the local bulk Reynolds number ranged from about 280 to 49,000, the local bulk Prandtl number varied from about 4 to 158, the local bulk Grashof number range was from 1000 to 2.5×10^5, and the local bulk Nusselt number varied from 13 to 258. The uniform wall average heat flux for the experiments ranged from about 4 to 670 kW/m^2. Heat balance errors were calculated for all experimental runs by taking a percent difference between two methods of calculating the heat addition. The product of the voltage drop across the test section and the current carried by the tube was the primary method, while the fluid enthalpy rise from inlet to exit was the second method. The heat balance error between the two methods in all cases was less than 5%. The primary method was the one used in the computer program [7] for all heat flux and heat transfer coefficient calculations.

The reliability of the flow circulation system and of the experimental procedures was checked by making several calibration runs with distilled water, and the results were compared with several of the well-established heat transfer correlations for fully developed turbulent pipe flow presented by Kakac et al [4]. The data were within $\pm 8\%$ of the predicted values. The uncertainty analyses of the overall experimental procedures using the method of Kline and McClintock [8] showed that there is a maximum of 9% uncertainty for heat transfer coefficient calculations and a maximum of 0.5% uncertainty for Reynolds number calculations. More detailed descriptions of the experimental apparatus and procedures may be found in Ref. 9.

FORCED AND MIXED CONVECTION HEAT TRANSFER BOUNDARY

Application of heat to the tube wall produces a temperature difference in the fluid. The fluid near the tube wall has a higher temperature and lower density than the fluid close to the centerline of the tube. This temperature difference may produce a secondary flow due to free convection. The boundary between mixed and forced convection can be determined from the local heat transfer data. The ratio of the local peripheral heat transfer coefficient at the top of the tube to the local peripheral heat transfer coefficient at the bottom of the tube (h_t/h_b) should be close to unity (0.8–1.0) for forced convection and is much less than unity (< 0.8) for a case in which mixed convection exists. Mixed convection heat transfer, in addition to being dependent on Reynolds and Prandtl numbers, is also dependent upon the Grashof number (which accounts for the variation in density of the test fluid).

To illustrate and explain the different heat transfer modes (mixed and forced convection) encountered for the three inlets during the experiments, Fig. 4 is presented. This figure shows the different trends in the heat transfer coefficient ratio h_t/h_b. It includes representative Reynolds number ranges from laminar to fully turbulent flow for

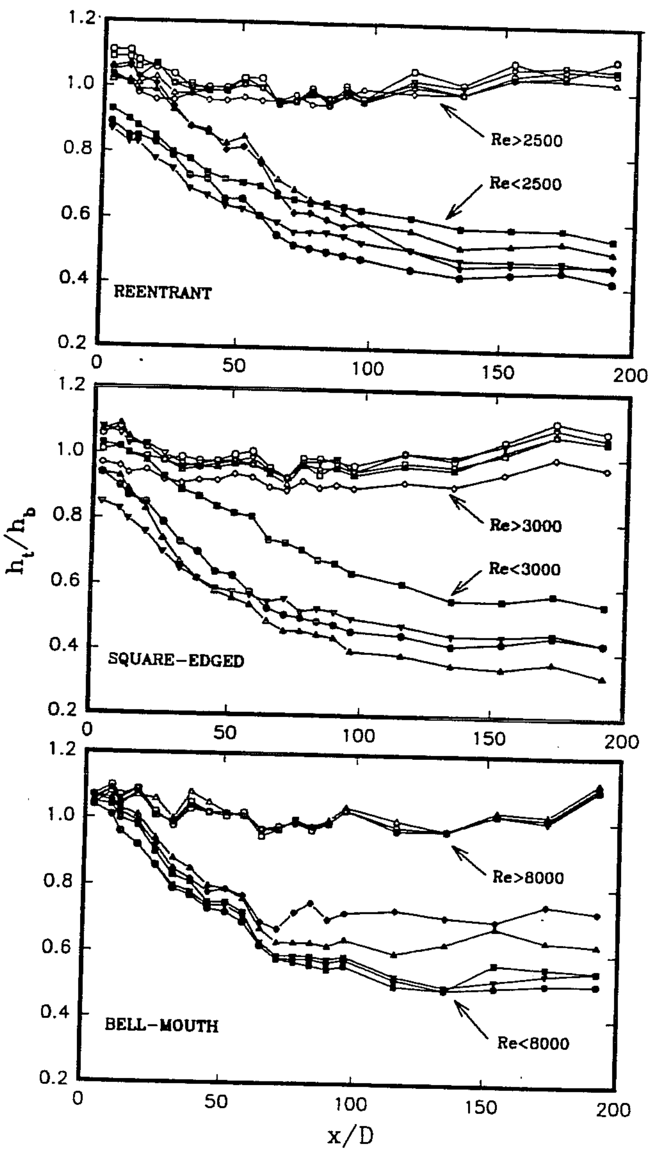

Figure 4. Effect of secondary flow on heat transfer coefficient for different inlets and flow regimes.

the three inlets (Re = 280–49,000). As shown in the figure, the boundary between forced and mixed convection heat transfer is inlet-dependent. For the reentrant, square-edged, and bell-mouth inlets when the Reynolds numbers were greater than 2500, 3000, and 8000, respectively, the flows were dominated by forced convection heat transfer and the heat transfer coefficient ratios did not fall below 0.8–0.9 and at times exceeded unity due to roundoff errors in the property evaluation subroutine of the data reduction program [7]. The flows dominated by mixed convection heat transfer had heat transfer coefficient ratios beginning near 1 but dropping off rapidly as the length-to-diameter ratio increased. Beyond about 125 diameters from the tube entrance, the ratio was almost invariant, with x/D indicating a much less dominant role for forced convection heat transfer and an increased free convection activity.

In reference to Fig. 4, it is interesting to observe that the starting length necessary for the establishment of the free convection effect for low Reynolds number flows was also inlet-dependent. When the secondary flow was established, a sharp decrease in h_t/h_b occurred. Depending on the type of inlet configuration, for low Reynolds number flows (Re < 2500 for reentrant, Re < 3000 for square-edged, and Re < 8000 for bell-mouth), the flow can be considered to be dominated by forced convection over the first 20–70 diameters from the entrance to the tube.

INFLUENCE OF INLET ON HEAT TRANSFER TRANSITION REGION

Figure 5 clearly shows the influence of inlet configuration on the beginning and end of the heat transfer transition region. This figure plots the local average peripheral heat transfer coefficients in terms of the Colburn j factor ($\mathrm{St}\,\mathrm{Pr}^{0.6}$) versus local bulk Reynolds number for all flow regimes at the length-to-diameter ratio of 192. The filled symbols represent the start and end of the heat transfer transition region for each inlet configuration. As shown by the filled symbols, the lower and upper limits of the heat transfer transition Reynolds number range are dependent on the inlet configuration.

Figure 5, for comparison purposes, also shows the typical fully developed pipe flow forced convection heat transfer correlations for turbulent [10] and laminar (Nu = 4.364) flows under the uniform wall heat flux boundary condition. In the turbulent flow regime, for Reynolds numbers greater than about 8500–10,500 (depending on the inlet type), the experimental data appear on the turbulent heat transfer line (within ±8%). However, in the laminar flow regime, for Reynolds numbers less than about 2000–3800 (depending on the inlet type), the data appear to have a pronounced and almost parallel shift above the accepted laminar heat transfer line. This is directly due to the strong influence of buoyancy forces (free convection) on forced convection (mixed convection), giving rise to mixed convection heat transfer. This in turn results in a higher fully developed laminar uniform wall heat flux Nusselt number than the accepted 4.364 value (a value of about 14.5 is estimated from the data). It should be noted that in the fully developed laminar flow region no forced convection data could be obtained. At the minimum welder current setting (approximately 150 A), the heat generated at the tube wall was enough to bring

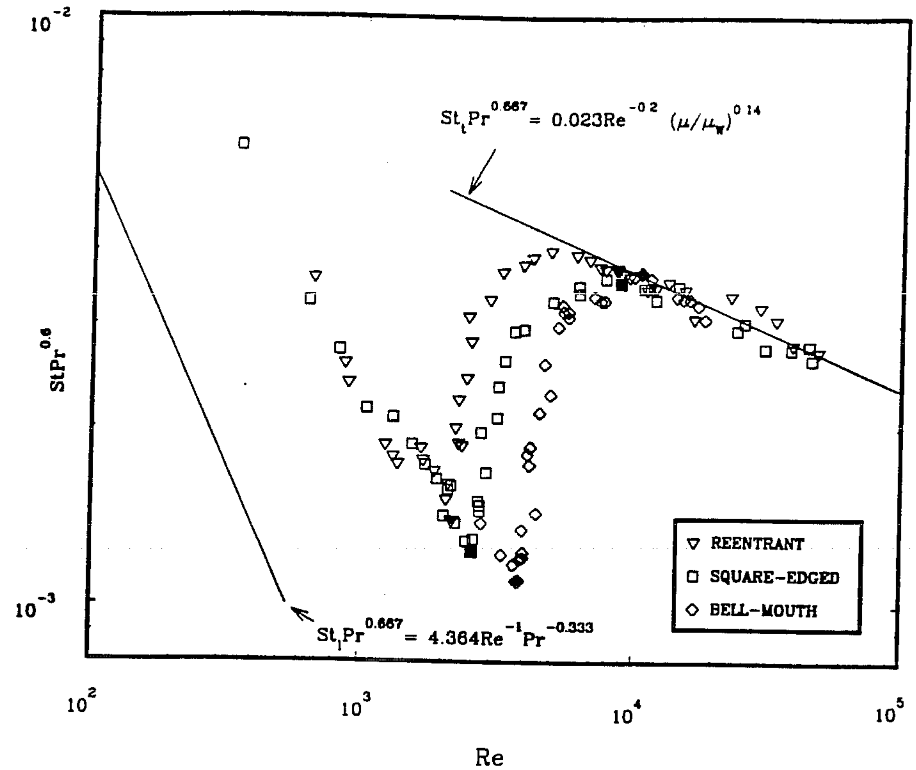

Figure 5. Influence of different inlets on heat transfer transition region at $x/D = 192$. (The solid symbols indicate the start and end of the transition region.)

about peripheral temperature variations extensive enough to cause secondary flow.

As shown by the filled symbols in Fig. 5, the lower and upper limits of heat transfer transition Reynolds number range depend on inlet configuration. In addition, these transition Reynolds number limits are x/D-dependent. Figure 4 demonstrates that after a certain length-to-diameter ratio (depending on the inlet), secondary flow will dominate. This is particularly true in the laminar and lower transition regions. The presence of the secondary flow and the fact that the wall and fluid bulk temperatures increase along the pipe cause the fluid kinematic viscosity to decrease with an increase in x/D. This in turn causes the local bulk Reynolds number (ie, lower and upper limits of heat transfer transition Reynolds number range) to increase along the pipe. To determine the range of heat transfer transition Reynolds number along the pipe ($3 \leq x/D \leq 192$), figures similar to Fig. 5 were developed for 20 other x/D locations. Figure 6 depicts the variation of the lower and the upper limits of heat transfer transition

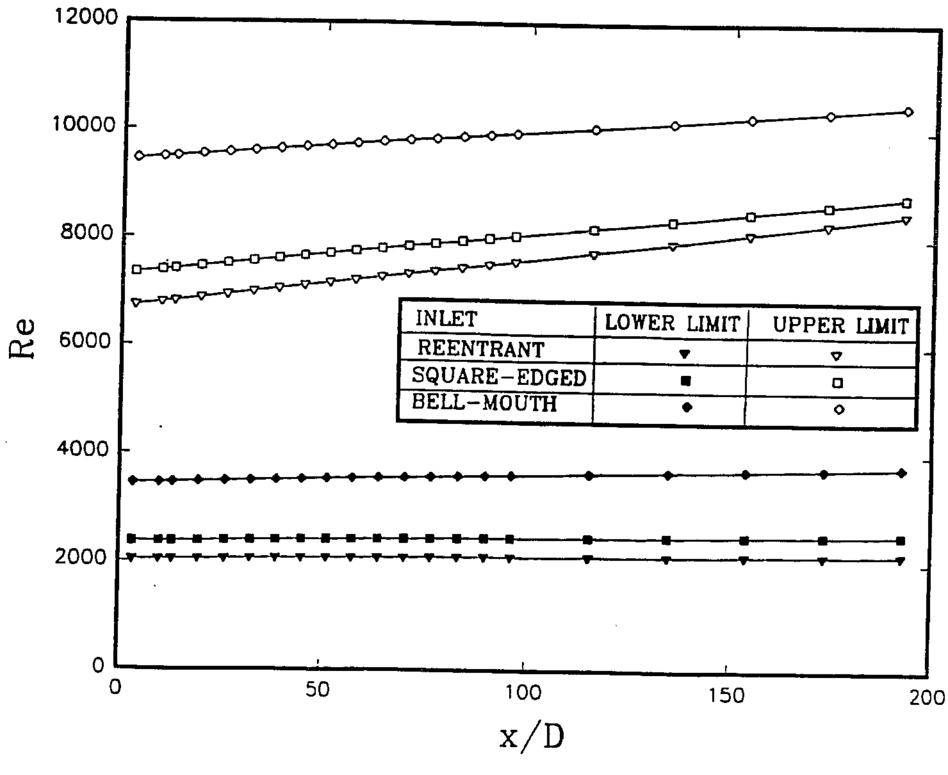

Figure 6. Variation of the lower and the upper limits of heat transfer transition Reynolds number along the pipe for different inlets.

Reynolds number along the pipe for each inlet. Based on the experimental results, the limits for the heat transfer transition Reynolds number range for each inlet over the entire tube ($3 \le x/D \le 192$) can be summarized as

Reentrant	$2000 < Re < 8500$
Square-edged	$2400 < Re < 8800$
Bell-mouth	$3800 < Re < 10{,}500$

The above limits for the heat transfer transition Reynolds number indicate that the inlet that caused the most disturbance (reentrant) produced an early transition (Re = 2000), and the inlet with the least disturbance (bell-mouth) did not go into transition below a Reynolds number of about 3800. The square-edged inlet, which cause less disturbance than the reentrant inlet but more than the bell-mouth inlet, produced a transition Reynolds number of about 2400. It should be pointed out that the reported lower (at $x/D = 3$) and upper (at $x/D = 192$) limits of heat transfer transition Reynolds number are not influenced by the presence of mixed convection (see Fig. 4). However, as the flow travels the pipe length required for the establishment of secondary flow, the beginning of the transition region will be influenced by the presence of mixed convection.

HEAT TRANSFER CORRELATION FOR THE LAMINAR REGION

As pointed out in reference to Fig. 4, the modes of heat transfer in the laminar flow region can be divided into forced and mixed convection. Pure forced convection can be observed near the entrance since secondary flow needs a certain length for development. To develop a heat transfer correlation in the entrance and fully developed laminar region, we used the mixed and forced convection data in this region. A correlation similar to the one proposed by Martinelli and Boelter [11] was curve-fitted to our data using a least squares curve-fitting program. The correlation is

$$Nu_l = 1.24\left[(Re\,Pr\,D/x) + 0.025(Gr\,Pr)^{0.75}\right]^{1/3}(\mu/\mu_w)^{0.14} \tag{1}$$

where

$$3 \le x/D \le 192, \quad 280 \le Re \le 3800, \quad 40 \le Pr \le 160,$$
$$1000 \le Gr \le 2.8 \times 10^4, \quad 1.2 \le \mu/\mu_w \le 3.8$$

Equation (1) is applicable to laminar forced and mixed convection in the entrance and fully developed regions and can be used for all three inlets. The equation gives a representation of the experimental data to within +15.4% and −16.9%. In the development of the correlation, a total of 546 experimental data points were used. The absolute average deviation between the results predicted by the correlation and the experimental data is 5.8%. About 14% of the data (78 data points) were predicted with more than ±10% deviation, and 86% of the data (468 data points) with less than ±10% deviation. Figure 7 compares the predicted Nusselt numbers obtained from Eq. (1) with measurements.

HEAT TRANSFER CORRELATION FOR THE TURBULENT REGION

In the turbulent flow region (refer to Fig. 4), the effect of free convection on our data is insignificant and the flow is considered to be dominated by forced convection effects. Using the entrance and fully developed turbulent forced convection data for all three inlets, a correlation similar to

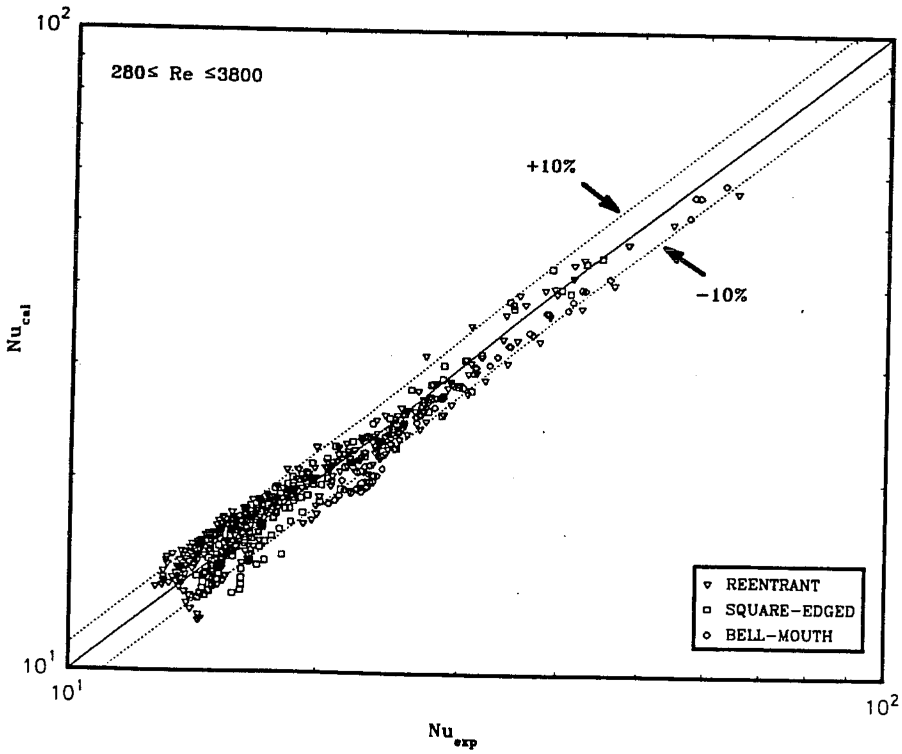

Figure 7. Comparison between experimental Nusselt numbers and those predicted by the proposed laminar region heat transfer correlation.

the Sieder and Tate correlation [10] was curve-fitted to our experimental data. The proposed correlation is

$$\mathrm{Nu}_t = 0.023\,\mathrm{Re}^{0.8}\,\mathrm{Pr}^{0.385}(x/D)^{-0.0054}(\mu/\mu_w)^{0.14} \quad (2)$$

where

$$3 \le x/D \le 192, \qquad 7000 \le \mathrm{Re} \le 49{,}000$$
$$4 \le \mathrm{Pr} \le 34, \qquad 1.1 \le \mu/\mu_w \le 1.7$$

Equation (2) is applicable to turbulent forced convection in the entrance and fully developed regions and can be used for all three inlets. The equation correlates the experimental data to within +10.5% and −10.3%. In the development of the correlation, 604 experimental data points were used. The absolute average deviation between the results predicted by the correlation and the experimental data is 3.7%. The correlation predicted 93% of the experimental data (600 data points) by less than ±10% deviation and 73% of the data with less than ±5% deviation. Figure 8 compares the Nusselt numbers obtained from Eq. (2) with measurements.

HEAT TRANSFER CORRELATION FOR THE TRANSITION REGION

In the transition region, flow has both laminar and turbulent characteristics. In addition, the type of inlet configuration influences the beginning and end of the transition region. Thus a single correlation for this region cannot predict the data, and a correlation for each inlet should be developed. The form of the correlation developed for this region is similar to the one proposed by Churchill [12] and is of the form

$$\mathrm{Nu}_{tr} = \{\mathrm{Nu}_l + \exp[(a - \mathrm{Re})/b] + \mathrm{Nu}_t^c\}^c \quad (3)$$

The equations for Nu_l and Nu_t are the same as Eqs. (1) and (2), respectively. Equation (3) was curve-fitted to our experimental data in the transition region, and the following constants were obtained for each inlet.

Reentrant

$$a = 1766, \qquad b = 276, \qquad c = -0.955$$

where

$$3 \le x/D \le 192, \qquad 1700 \le \mathrm{Re} \le 9100, \qquad 5 \le \mathrm{Pr} \le 51$$
$$4000 \le \mathrm{Gr} \le 2.1 \times 10^5, \qquad 1.2 \le \mu/\mu_w \le 2.2$$

Square-edged

$$a = 2617, \qquad b = 207, \qquad c = -0.950$$

where

$$3 \le x/D \le 192, \qquad 1600 \le \mathrm{Re} \le 10{,}700, \qquad 5 \le \mathrm{Pr} \le 55$$
$$4000 \le \mathrm{Gr} \le 2.5 \times 10^5, \qquad 1.2 \le \mu/\mu_w \le 2.6$$

Bell-mouth

$$a = 6628, \qquad b = 237, \qquad c = -0.980$$

where

$$3 \le x/D \le 192, \qquad 3300 \le \mathrm{Re} \le 11{,}100, \qquad 13 \le \mathrm{Pr} \le 77$$
$$6000 \le \mathrm{Gr} \le 1.1 \times 10^5, \qquad 1.2 \le \mu/\mu_w \le 3.1$$

Equation (3) is applicable to transition forced and mixed convection in the entrance and fully developed regions and should be used with an appropriate set of constants for each inlet configuration. For the development of the transition region correlation for the reentrant inlet, 441 experimental data points were used. The correlation gave a representation of the experimental data to within +25.1% and −23% and had an absolute average deviation of 8%. Three percent of

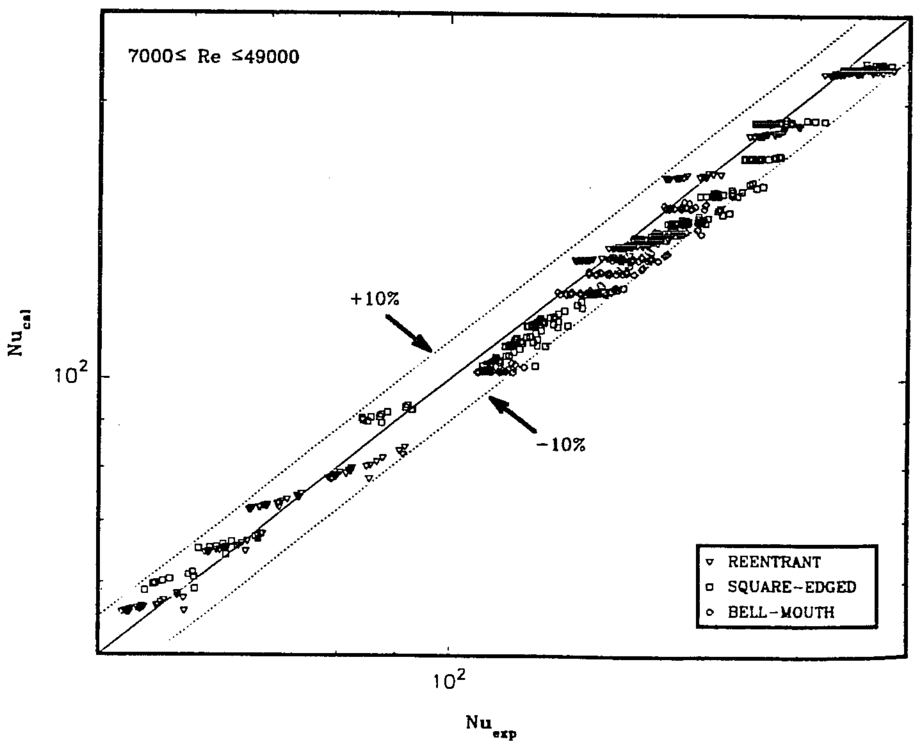

Figure 8. Comparison between experimental Nusselt numbers and those predicted by the proposed turbulent region heat transfer correlation.

the data (13 data points) were predicted with more than $\pm 20\%$ deviation, 29% (129 data points) with ± 10–20% deviation, and 68% (299 data points) with less than $\pm 10\%$ deviation. For the square-edged inlet, 416 experimental data points were used for the development of the correlation. The equation correlated the experimental data to within $+24.3\%$ and -23.9% and had an absolute average deviation of 7.2%. Three percent of the data (12 data points) were predicted with more than $\pm 20\%$ deviation, 26% (106 data points) with ± 10–20% deviation, and 72% (298 data points) with less than $\pm 10\%$ deviation. The correlation for the bell-mouth inlet was based on 433 experimental data points. The correlation represented the experimental data to within $+18.5\%$ and -22% and had an absolute average deviation of 8.1%. Less than 1% of the data (four data points) were predicted with more than -20% deviation, 24% (104 data points) with ± 10–20% deviation, and 75% (325 data points) with less than $\pm 10\%$ deviation. Figure 9 compares the predicted Nusselt numbers obtained from Eq. (3) for each inlet with measurements.

In summary, five new forced and mixed heat transfer correlations for the three inlets have been developed corresponding to the entrance and fully developed data for each flow region. Common correlations were used in the laminar [see Eq. (1)] and turbulent [see Eq. (2)] regions for the three inlets. Because the transition region is dependent on inlet configuration, three separate correlations were developed in the transition region, one for each inlet. To have a continuous prediction from the proposed correlations for each inlet across all flow regimes, the limits of each correlation were stretched as much as possible without loss of accuracy into the other regions.

COMPARISON OF AVAILABLE CORRELATIONS WITH EXPERIMENTS

A large number of fully developed forced convection heat transfer correlations for pipes with a rounded entrance have been compared by Shah and Johnson [2], and these comparison have been extended by Kakac et al [4]. Based on these extensive comparisons, the following fully developed forced convection correlation developed by Gnielinski [13] for $2300 \leq \text{Re} \leq 5 \times 10^4$ and $0.5 \leq \text{Pr} \leq 2000$ was recommended:

$$\text{Nu} = \frac{(f/2)(\text{Re} - 1000)\text{Pr}}{1 + 12.7(f/2)^{0.5}(\text{Pr}^{2/3} - 1)}$$

where

$$f = (1.58 \ln \text{Re} - 3.28)^{-2}$$

Gnielinski's correlation was compared with our fully developed forced convection heat transfer data in the transition and turbulent regions for all three inlets (see Fig. 10). The correlation predicted our experimental data within $\pm 20\%$. Since Gnielinski's correlation was based on experimental data for a smooth entrance (bell-mouth), the accuracy of the correlation improved to well within $\pm 10\%$ for this inlet.

Another correlation recommended by Kakac et al [4] was the one developed by Churchill [12]. This correlation is based on asymptotic solutions/correlations and was constructed for $0 < \text{Pr} < 10^6$ and $10 \leq \text{Re} \leq 10^6$, spanning the laminar, transition, and turbulent flow regimes.

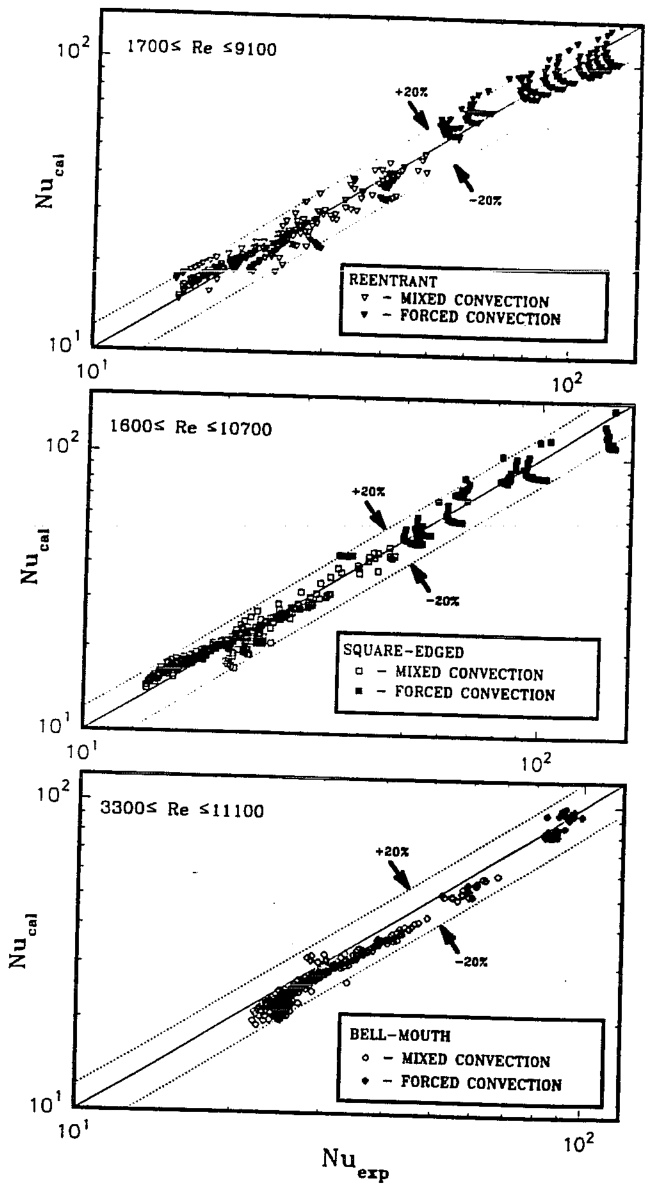

Figure 9. Comparison between experimental Nusselt numbers and those predicted by the proposed transition region heat transfer correlation.

Churchill's correlation is restricted to fully developed forced convection heat transfer in pipes with a rounded entrance. The correlation for uniform wall heat flux boundary condition is of the form

$$\text{Nu}^{10} = \text{Nu}_l^{10} + \left[\frac{\exp[(2200 - \text{Re})/365]}{\text{Nu}_l^2} + \frac{1}{\text{Nu}_t^2}\right]^{-5}$$

where

$$\text{Nu}_l = 4.364 \qquad \text{and } \text{Nu}_t = 6.3 + \frac{0.079(f/2)^{1/2}\text{Re Pr}}{(1 + \text{Pr}^{4/5})^{5/6}}$$

Churchill's correlation was compared with our fully developed forced convection heat transfer data for all three inlets (see Fig. 11). For the bell-mouth inlet, the correlation predicted our experimental data within $\pm 10\%$.

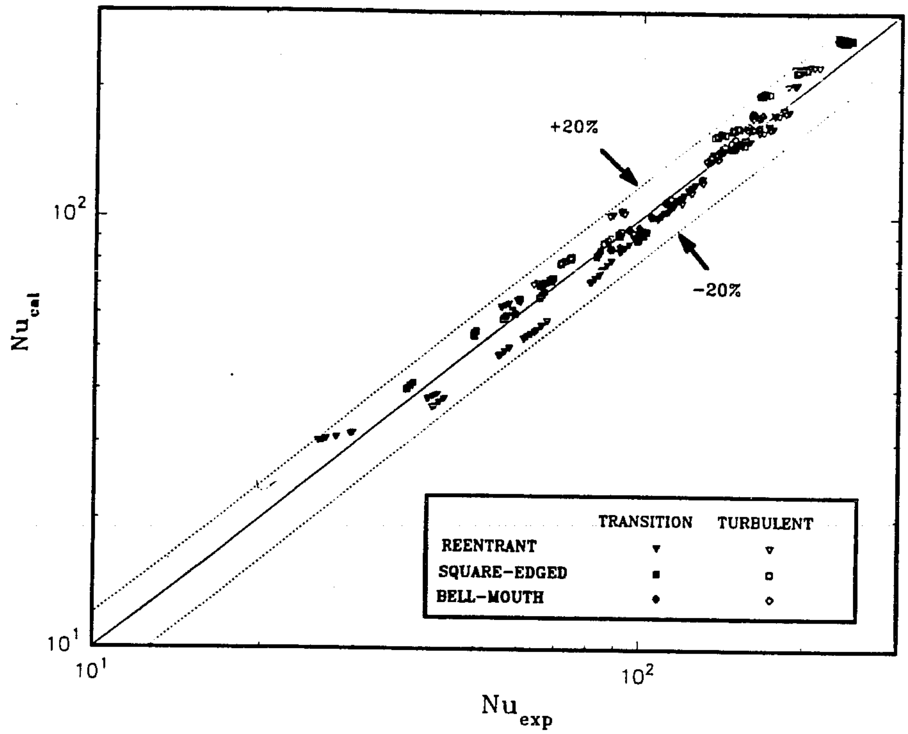

Figure 10. Comparison between experimental fully developed forced convective heat transfer data for all three inlets and correlation of Gnielinski [13].

However, for the other two inlets the predictions were not as accurate. For Re > 4000 the correlation predicted the reentrant and square-edged data with an accuracy of $\pm 30\%$. For Re < 4000 the accuracy of the correlation deteriorated with a decrease in the Reynolds number, and the correlation underpredicted the experimental data by 40–80%. This was due to the strong influence of inlet configuration on the heat transfer coefficient in the laminar and lower transition regions, which was not accounted for in Churchill's correlation.

The comparisons shown in Figs. 10 and 11 indicate that the correlations do a good job of predicting fully developed forced convection Nusselt numbers in the upper transition and turbulent regions for different inlets. The accuracy of the predictions improved when the correlations were compared with the data for a rounded entrance

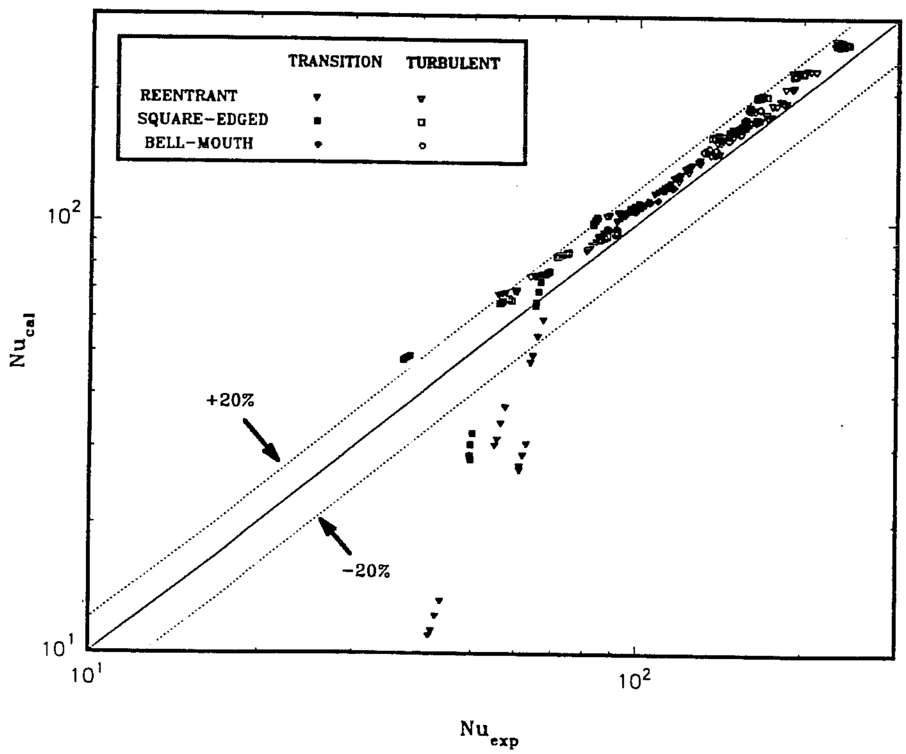

Figure 11. Comparison between experimental fully developed forced convective heat transfer data for all three inlets and correlation of Churchill [12].

(bell-mouth). However, the correlations have a limited range of application and cannot be applied to flows where mixed convection, inlet, and entrance effects are important. For these flows the correlations developed in this study are recommended; see Eqs. (1)–(3).

It should be noted that the experimental data in the laminar and transition regions for the reentrant and square-edged inlets were also compared with other correlations presented in Kakac et al [4], and the results of these comparisons showed no clear trend (see Refs. 14 and 15). For a given flow regime, no single correlation predicted the respective experimental data with any consistency. This was particularly true for the mixed laminar and lower transition regions. This lack of prediction was attributed to the strong influence of secondary flow and the shape of inlet configuration on the heat transfer coefficient in these regions.

PRACTICAL SIGNIFICANCE

The type of inlet configuration significantly influences the establishment of secondary flow, the development of the heat transfer coefficient along the pipe, and the beginning and end of the heat transfer transition region. The heat transfer correlations provided in this study can be used to assist the heat exchanger designer in predicting the heat transfer coefficient along a horizontal straight circular tube with uniform heat flux for a specified inlet configuration in all flow regimes. The proposed correlations also offer a valuable tool for verification of the computational codes. Once the codes have been verified they can be used to improve design and to gain a better understanding of the physics of the flow under actual operating conditions.

SUMMARY AND CONCLUSIONS

This study provided an extensive and accurate heat transfer database across all flow regimes in the entrance and fully developed regions for three different inlet configurations. Both forced and mixed convection modes of heat transfer were studied. The heat transfer results for the three inlets showed that the range of Reynolds number values for which transition flow exists is strongly inlet-dependent. The establishment of secondary flow along the pipe also proved to be inlet configuration dependent. In the laminar and lower transition flow regions, mixed convection was found to be the dominant mode of heat transfer. In the turbulent region, the influence of free convection was found to be negligible, and inlet configuration had a minor influence on the heat transfer coefficient. The boundary between forced and mixed convection also showed a strong dependency on the inlet configuration.

Based on the obtained experimental data, heat transfer correlations capable of predicting both entrance and fully developed forced and mixed convection heat transfer coefficients in the laminar, transition, and turbulent flow regimes were developed. These correlations are unique in the sense that they include the significant influences of different inlet configurations on the heat transfer coefficient along the pipe. These influences are more pronounced in the laminar and transition region correlations.

Comparison of our fully developed forced convection heat transfer data in the transition and turbulent regions for a bell-mouth inlet showed excellent agreement with the correlations developed by Gnielinski [13] and Churchill [12]. However, the accuracy of these correlations deteriorated as the influence of inlet configuration on the heat transfer coefficient became more pronounced. Therefore, caution should be exercised in applying these correlations to tubes with distributed entrances (reentrant and square-edged). In addition, none of the reported correlations in the literature were capable of predicting our entrance and fully developed mixed convective heat transfer data for disturbed entrances in the laminar and transition regions with any consistency. For these flows the correlations developed in this study are recommended.

Support for this research was provided by the National Science Foundation under grant number CBT-8813342.

NOMENCLATURE

- c_P specific heat of the test fluid evaluated at T_b, J/(kg · K)
- D inside diameter of test section (tube), m
- f fully developed Fanning friction factor, dimensionless
- g acceleration of gravity, m/s^2
- h local average or fully developed peripheral heat transfer coefficient [$= \dot{q}_i''/(T_{wi} - T_b)$], W/(m^2 · K)
- h_b local peripheral heat transfer coefficient at the bottom of the tube, W/(m^2 · K)
- h_t local peripheral heat transfer coefficient at the top of the tube (180° from h_b), W/(m^2 · K)
- h_x local peripheral heat transfer coefficient [$= \dot{q}_{ix}''/(T_{wix} - T_b)$], W/(m^2 · K)
- Gr local bulk Grashof number [$= g\beta\rho^2 D^3(T_{wi} - T_b)/\mu^2$], dimensionless
- k thermal conductivity of the test fluid evaluated at T_b, W/(m · K)
- L length of the test section (tube), m
- Nu local average or fully developed peripheral Nusselt number ($= hD/k$), dimensionless
- Nu_l local average or fully developed peripheral laminar Nusselt number, dimensionless
- Nu_t local average or fully developed peripheral turbulent Nusselt number, dimensionless
- Nu_{tr} local average or fully developed peripheral transitional Nusselt number, dimensionless
- Nu_x local peripheral Nusselt number ($= h_x D/k$), dimensionless
- Pr local bulk Prandtl number ($= \mu c_P/k$), dimensionless
- $\dot{q}_i''$ local average peripheral inside wall heat flux, W/m^2
- $\dot{q}_{ix}''$ local peripheral tube inside wall heat flux, W/m^2
- Re local bulk Reynolds number ($= \rho VD/\mu$), dimensionless
- St local average or fully developed peripheral Stanton number [= Nu/(Pr Re)], dimensionless
- T_b local bulk temperature of the test fluid, °C
- T_{wi} local average peripheral tube inside wall temperature, °C
- T_{wix} local peripheral tube inside wall temperature, °C

V average velocity in the test section, m/s
x local distance along the test section from the inlet, m

Greek Symbols

β coefficient of thermal expansion of the test fluid evaluated at T_b, K^{-1}
μ absolute viscosity of the test fluid evaluated at T_b, Pa · s
μ_w absolute viscosity of the test fluid evaluated at T_{wi}, Pa · s
ρ density of the test fluid evaluated at T_b, kg/m^3

REFERENCES

1. Shah, R. K., and London, A. L., *Laminar Flow Forced Convection in Ducts*, a supplement to *Advances in Heat Transfer*, Academic, New York, 1978.
2. Shah, R. K., and Johnson, R. S., Correlations for Fully Developed Turbulent Flow Through Circular and Noncircular Channels, Sixth Nat. Heat and Mass Transfer Conf., Indian Inst. Technology, Madras, India, pp. D-75–D-95, 1981.
3. Kakac, S., Shah, R. K., and Bergles, A. E., *Low Reynolds Number Flow Heat Exchangers*, Hemisphere, New York, 1981.
4. Kakac, S., Shah, R. K., and Aung, W., *Handbook of Single-Phase Convective Heat Transfer*, Wiley, New York, 1987.
5. Ghajar, A. J., and Madon, K. F., Pressure Drop Measurements in the Transition Region for a Circular Tube with Three Different Inlet Configurations, *J. Exp. Thermal Fluid Sci.*, 35(8), 1927–1934, 1992.
6. Morel, T., Comprehensive Design of Axisymmetric Wind Tunnel Contractions, *Trans. ASME J. Fluids Eng.*, 97, 225–233, 1975.
7. Ghajar, A. J., and Zurigat, Y. H., Microcomputer-Assisted Heat Transfer Measurement/Analysis in a Circular Tube, *J. Appl. Eng. Educ.*, 7(2), 125–134, 1991.
8. Kline, S. J., and McClintock, F. A., Describing Uncertainties in Single Sample Experiments, *Mech. Eng.*, 75(1), 3–8, 1953.
9. Strickland, D. T., Heat Transfer Measurements in the Transition Region for a Horizontal Circular Tube with a Square-Edged Entrance, M.S. Thesis, Oklahoma State Univ., Stillwater, 1990.
10. Sieder, E. N., and Tate, G. E., Heat Transfer and Pressure Drop in Liquids in Tubes, *Ind. Eng. Chem.*, 28, 1429–1435, 1936.
11. Martinelli, R. C., and Boelter, L. M. K., The Analytical Prediction of Superposed Free and Forced Viscous Convection in a Vertical Pipe, *Univ. Calif. Publ. Eng.*, 5(2), 23, 1942.
12. Churchill, S. W., Comprehensive Correlating Equations for Heat, Mass and Momentum Transfer in Fully Developed Flow in Smooth Tubes, *Ind. Eng. Chem. Fundam.*, 16(1), 109–116, 1977.
13. Gnielinski, V., New Equations for Heat and Mass Transfer in Turbulent Pipe and Channel Flow, *Int. Chem. Eng.*, 16, 359–368, 1976.
14. Ghajar, A. J., and Strickland, D. T., Forced and Mixed Convective Heat Transfer Correlations in the Laminar-Transition-Turbulent Regions for a Circular Tube with a Square-Edged Entrance, Presented at the AIAA/ASME 5th Joint Thermophysics Conference, Seattle, AIAA Paper No. 90-1762, 1990.
15. Ghajar, A. J., Strickland, D. T., and Kuppuraju, S., Forced and Mixed Convective Heat Transfer Measurements in a Circular Tube with Different Inlets, in *Mixed Convection*, R. L. Mahajan and R. D. Boyd, Eds., HTD-Vol. 152, 37–45, ASME, New York, 1990.

Received November 5, 1992; revised September 20, 1993